MARTIN MARIETTA ENERGY SYSTEMS LIBRARIES

3 4456 0316322 5

ORNL/TR-90/21

MEASUREMENT OF THE MOMENTUM PRESSURE DROP AND STUDY OF THE APPEARANCE OF VAPOR AND CHANGE IN THE VOID FRACTION IN SUBCOOLED BOILING AT LOW PRESSURE

Prepared for the

OAK RIDGE NATIONAL LABORATORY
Oak Ridge, Tennessee 37831
operated by
MARTIN MARIETTA ENERGY SYSTEMS, INC.
for the
U.S. DEPARTMENT OF ENERGY
under Contract No. DE-AC05-84OR21400

Translated from French by the Ralph McElroy Co., Custom Division
P. O. Box 4828, Austin, Texas 78765 USA

OAK RIDGE NATIONAL LABORATORY
CENTRAL RESEARCH LIBRARY
CIRCULATION SECTION
4500N ROOM 175
LIBRARY LOAN COPY
DO NOT TRANSFER TO ANOTHER PERSON
If you wish someone else to see this report, send in name with report and the library will arrange a loan.
UCN-7969 (3 9-77)

Code: 691-4968

Center of Nuclear Studies of Grenoble
Department of Heat Transfers

MEASUREMENT OF THE MOMENTUM PRESSURE DROP AND STUDY OF THE APPEARANCE OF VAPOR AND CHANGE IN THE VOID FRACTION IN SUBCOOLED BOILING AT LOW PRESSURE

J. Costa

Communication presented at the Meeting of the European Group Double-Phase - WINFRITH - 1967

MARTIN MARIETTA ENERGY SYSTEMS LIBRARIES

3 4456 0316322 5

The momentum pressure drop, in subcooled boiling at low pressure, is determined by the use of the recovery of pressure which follows the vapor condensation in the non heated length of a channel of uniform cross-section.

Two parts can be distinguished in subcooled boiling :

- a highly subcooled one where the void fraction is negligible
- a slightly subcooled one where the void fraction is important.

The "point of net vapor generation" is correlated, from our results, by : $\theta = K\,\varphi/\sqrt{V}$ with

θ = subcooling (°C)
K = empirical constant (1,8 for circular channel ; 1,28 for rectangular channel)
φ = heat flux (W/cm^2)
V = single phase velocity (cm/s)

A void fraction model is derived from the correlation $\theta = K\,\varphi\,\sqrt{V}$.

The parameters range is :

geometry : rectangular channel : 600 × 38 × 2 and 600 × 38 × 3,6 mm
Circular channel : 6 mm I.D
pressure : from 1,75 to 5 bars abs
flow rate : from 300 to 700 $g/cm^2.s$
heat flux : from 100 to 400 W/cm^2.

Table of Contents

0. Introduction
1. Experimental device
2. Interpretation of a type result
3. Method for measuring the momentum pressure drop in subcooled boiling
4. Applications of the method
   4.1 Appearance of the vapor in subcooled boiling
   4.2 Change of the void [fraction] in subcooled boiling
5. Conclusion

Notations

B	=	perimeter of exchange between vapor and liquid
B_C	=	heated perimeter
C	=	specific heat of the water
G	=	mass velocity
K	=	empirical constant: 1.8 for the channel with 6 ϕ [sic; 6 mm ϕ] and 1.28; for the rectangular channels of 2 and 3.6 mm
L	=	heated length
L	=	latent heat of vaporization of the water
M	=	mass flow rate
m	=	empirical constant: 2
n	=	empirical constant: 1
P	=	pressure
P_S	=	pressure at the end of the heated length
T_E	=	temperature of entrance
T_{pm}	=	temperature of moistened wall
T_{FG}	=	Forster and Greiff temperature = $T_{sat} + \Delta T_{FG}$
T_{colb}	=	temperature calculated with the formula of Colburn
T_S	=	temperature of outlet
T_{sat}	=	temperature of saturation
T_L	=	average temperature of the liquid
T	=	temperature of heat balance = T_F ?
T_o	=	temperature of heat balance for $z = 0$
V	=	velocity (cm/s)
V_L	=	velocity of the liquid
V_G	=	velocity of the vapor

W_T	=	power supplied to the channel per unit of length
W_V	=	power absorbed by the vaporization per unit of length
x	=	vapor titer
z	=	abscissa
ΔP	=	pressure drop
ΔP_{acc}	=	momentum pressure drop
ΔT_{FG}	=	superheating calculated by the simplified Forster and Greiff formula
α	=	average void fraction
α_0	=	average void fraction for $T = T_{sat}$
β	=	$\rho V/\rho L$
γ	=	V_G/V_L
δ		1 if $T_{colb} \geq T_{sat}\ T_{FG}$ 0 if $T_{colb} < T_{sat} + T_{FG}$
ρV	=	specific mass of the vapor
ρL	=	specific mass of the liquid
ξ	=	$\overline{G^2}/\overline{G^2}$
ϕ	=	heat flux (W/cm^2)
θ	=	undersaturation with the appearance of the vapor = $T_{sat} - T_L$ (°C)

<u>List of figures</u>

No. 1 Diagram of the loop

2 Diagram of the rectangular test section

3 Type result

4	Momentum pressure drop as a function of the temperature of outlet
5	Influence of the state of the surface of the channel
6	Influence of the heated length and of the gas content on the appearance of vapor in subcooled boiling
7	Influence of the heated length and of the gas content on the superheating in subcooled boiling
8A and 8B	Comparison of the experimental results with the Bowring formula
9A and 9B	Correlation of the experimental results
10	Comparison: calculated void fraction and measured void fraction
11	Condensation at the end of heated length

0. Introduction

Numerous experiments have been performed to study pressure drop in subcooled boiling because knowledge of these drops is absolute necessary for heat calculations of the nuclear reactors which are cooled with water and particularly for research reactors at low pressure.

The results of these tests are presented, in general, in the form of networks of curves in terms of S (ΔP as a function of M for set T_E, ϕ, P_S). The minimum of these curves is the point to be determined because this is the point which conditions the appearance of the phenomenon of redistribution of flow rate between the hot channels and the cold channels at the core [1].

Some correlations give the flow rate of redistribution [2], and others give the total pressure drops in subcooled boiling [3,4].

Most of these experiments were done with a uniform flux, others with a flux varying longitudinally or transversely or even with double-heat generator [1] in order to approximate the real conditions of the reactor. But to our knowledge, no manipulation has been performed in order to study the variations in pressure connected to a discontinuity of flux, in particular the passage from flux ϕ to a flux of zero in a channel with constant cross section. These conditions exist at the ends of fuel plates because the active part containing the uranium is stopped at a few centimeters from the end of the plates.

We have therefore constructed a test section with a heated length followed by a nonheated length, and we have measured the recovery of pressure which accompanies the condensation of the

vapor in the nonheated part downstream. The measurements have enabled one to separate the momentum pressure drop from the total pressure drop, to study the conditions of appearance of the vapor and the change in the void fraction in subcooled boiling.

1. Experimental device

The test section, either rectangular (Figure 2) or circular, was mounted on a loop of which the diagram is given (Figure 1).

Per test, we measured:

- the pressure at different outlets located over the heated length and over the nonheated length*
- the temperature of the dry wall over the heated length
- the temperatures of entrance and of exit of the water
- the flow rate
- the power supplied to the channel

The parameter range studied was the following:

Pressure: 1.75 - 3 - 5 absolute bar

Flux: from 100 to 400 W/cm^2

Flow rate: from 3 to 7 m/sec

Geometry: rectangular channel 38 x 3.6 x 600 mm
rectangular channel 38 x 2 x 600 mm
circular channel 6 ϕ, length 600 to 120 mm

Degassed water: $\simeq$0.2 ppm.

---

*In order to avoid boiling in the pressure outlets, they were cooled.

2. Interpretation of a representative result

Figure 3 represents the reading of the measured values for a flow in subcooled boiling in the 3.6 mm rectangular channel.

Why does the pressure rise in zone 4 of the flow, that is to say downstream from the heated length?

An inspection glass located in zone 4 of recovery of pressure enables us to see that there is condensation of vapor: the vapor was formed in undersaturated boiling in the heated part of the channel, and it condenses downstream, in the nonheated part, because it is in thermodynamic nonequilibrium.

This condensation is accompanied by a recovery of pressure in the same manner as the creation of vapor in a channel is accompanied by a momentum pressure drop:

Let us calculate the difference in pressure between a section of the channel where the void fraction is zero ($P_{(o)}$) and a section where the void fraction is α | ($P_{(\alpha)}$) (not taking into account the pressure drops by friction and elevation) [sic; temperature increase]. Application of the theorem of the quantities of movement leads to:

$$- P_{(o)} - P_{(\alpha)} = \frac{G^2}{\rho_L}\left(\frac{\alpha}{1 - \alpha}\right) \qquad (1)$$

assuming the velocity profile of the liquid to be flat and neglecting the quantity of movement of the vapor

$$- P_{(o)} - P_{(\alpha)} = \frac{G^2}{\rho_L} \cdot \left(\frac{1 - \alpha + \alpha\beta\gamma^2 - (1 - \alpha + \alpha\beta\gamma)^2}{(1 - \alpha + \alpha\beta\gamma)^2}\right)$$

letting

$\gamma = \frac{V_G}{V_L}$ $\beta = \frac{\rho_G}{\rho_L}$ that is to say taking into account the quantity of movement of the vapor.

$$- P_{(o)} - P_{(\alpha)} = \frac{\bar{G}^2}{\rho_L} \left(\frac{\xi_\alpha - \xi_o + \alpha \xi_o}{1 - \alpha} \right)$$

neglecting the vapor and taking into consideration the velocity profile of the liquid.

Let us consider formula (1): we see that in order to pass from a section of the flow where the void fraction is zero to a section where the void fraction is α, the pressure decreases by

$$\left(\frac{\alpha}{1 - \alpha} \right)$$

and in order to pass from α to 0, the pressure rises by

$$\left(\frac{\alpha}{1 - \alpha} \right).$$

<u>Conclusion</u>: The recovery of pressure in zone 4 gives us information concerning the momentum pressure drop and the void fraction at the end of the heated length of the channel.

3. A method for measuring the momentum pressure drop in subcooled boiling

The formulas established in §II do not take into account the pressure drops by friction and by elevation; therefore, we cannot obtain the momentum pressure drop except by an approximate manner. In Figure 3: let us extrapolate the piezometric line of zone 5 towards the end of the heated length. The difference in pressure ΔP_{acc}^{min} is a value which is less than the real pressure recovery because the gradients of pressure drop by friction in zone 4 are greater than those of zone 5 (zone 4 double phase, zone 5 single phase).

Let us extrapolate the piezometric line from zone 2 towards the end of the heated length. The difference in pressure ΔP_{acc}^{max} is a value which is greater than the real pressure recovery because the gradients of pressure drop by friction in zone 3 are greater than those of zone 2 (zone 3 double phase, zone 2 single phase).

Conclusion: $$\Delta P_{acc}^{min} < \Delta P_{acc} < \Delta P_{acc}^{max}$$

This inequality gives, at the same time, the maximum uncertainty of the measurement. We can obtain a more likely value of ΔP_{acc} by graphically estimating the line of the pressure drop by friction and elevation in zones 3 and 4 between the two extrapolations of the piezometric lines upstream and downstream.

The limits of this method depend on the desired precision and the test conditions. In the range of parameters studied, the method gave us good results.

For the low void fractions with high undersaturation the precision is satisfactory because the condensation occurs over a short distance. It is in this zone that the measurements of void fractions by absorption of radiation (γ or α) are the least precise.

For the temperatures of outlet which are near saturation, the length of condensation is great. In order to improve the precision, we accelerated the condensation by injecting, at the end of the heated length through a pressure outlet, an output (a few % of the output of the channel) of cold water. We were thus able to measure the momentum pressure drop up to thermodynamic titers of zero in outlet of the heated length.

A method exists for measuring the quantity of movement, which consists of measuring the thrust on a T [5]. This method has a general use because it enables measurements in free [sic] boiling and measurements on a double-phase flow with two constituents, but there are difficulties with regard to the critical flow rates.

4. Applications of the method

4.1 Study of the appearance of vapor in subcooled boiling

4.1.1 The point of appearance of vapor

Let us consider a series of tests at the same pressure at the end of the heated length P_S, the same heat flux, and the same flow rate, but with different temperatures of outlets, and let us measure for each test, the momentum pressure drop using the method of §3.

Figure 4 shows the values of the momentum pressure drop and of the temperature of the wall at the end of the heated length.

We see that the momentum pressure drop, therefore the vapor, appears suddenly. This is the point of appearance of the vapor or "point of net vapor generation" that Zuber and Staub [7] and Bowring [6] previously studied, the point which we define as the intersection of the axis of the temperatures with the line representing the momentum pressure drop. Let us note that the determination of this point is practically independent from the method of measurement of the momentum pressure drop since it is not the exact value which interests us but only the conditions under which it appears.

This points divides the zone of flow in subcooled boiling into two parts:

- a highly undersaturated zone where the temperature of the wall progressively diverges from the value that it would have in forced convection in single phase in order to reach a stage above the temperature of saturation.

In this zone, the void fraction is very low because the bubbles remain at the wall.

- a weakly undersaturate zone where the void fraction is great because the vapor bubbles are detached and infest the core of the flow.

We have established that in this zone, the temperature of the wall has a tendency to decrease a few degrees with respect to its value in the highly undersaturated zone.

4.1.2 Influence of the state of the surface channel on the conditions of appearance of vapor

A series of tests done on the circular channel with 6 mm ϕ, after a campaign of one month, was redone after cleaning the channel.

Comparison of the two series of tests gives the following results (see Figure No. 5):

- in single phase, the temperature of the moistened wall is unchanged
- in highly undersaturated boiling the temperature of the wall is less by approximately 10°C for the tests after cleaning
- in weakly undersaturated boiling the difference between the temperatures of the wall decreases (5°C)
- the fluid temperature for which the recovery of pressure appears is unchanged
- the total pressure drops of the test after cleaning are higher by 2% than those of the preceding test.

Interpretation

We can interpret the results in the following way: on the moistened wall of the channel, the seeds [= K[illegible]] of boiling are more numerous after than before cleaning: in effect, after a campaign of tests of one month in degassed water, a great number of small pockets of air contained in the irregularities of the surface have disappeared and putting the channel in contact with air reproduces them.

Consequently, for the channel after cleaning, the seeds of boiling are more numerous; therefore, the temperature of the wall is lower; therefore, the pressure drops by friction are greater.

4.1.3 Influence of the heated length on the conditions of appearance of the vapor

We performed a series of tests at the same pressure, flux, and flow rate but with heated lengths of 600, 300, 217 and 113 mm; the results are shown in Figures 6 and 7.

It results from this that the heated length, in the range of variations studied, has practically no influence on the conditions of appearance of the vapor in subcooled boiling but, in contrast, modifies considerably the superheating of the wall.

4.1.4 Influence of the content of dissolved gas in water on the conditions of appearance of vapor

We performed a test with water whose gas content was 4 ppm, and we compared the results with those of the same tests with degassed water (0.2 ppm) (see Figures 6 and 7).

It results from this that the gas content has no influence on the conditions of appearance of vapor in subcooled boiling but, in contrast, modifies the superheating at the wall.

4.1.5 Results - Comparison with the Bowring formula

According to paragraphs 4.1.2, 4.1.3, and 4.1.4, we see that the conditions of appearance of vapor in subcooled boiling do not depend on the wall and seem only to be a function of the overall values of the flow, namely: the flux, the velocity, the undersaturation.

Table I gives the results of our tests.

In Figures 8A and 8B, we compared our results with those given by the Bowring formula: $V\theta/\phi = 14 + 0.1P$. It seems that, for a given velocity, θ is indeed proportional to ϕ but that for a given flux, θ is not inversely proportional to V. In Figures 9A and 9B, we give θ as a function of

$$\varphi/\sqrt{V}$$

and since the dispersion is low (±2°C) we therefore propose a correlation with the form:

$$\frac{\sqrt{V}.\theta}{\varphi} = K \qquad \text{K depends on the geometry}$$

K = 1.8 for the circular channel with 6 mm ϕ

K = 1.28 for the rectangular 2 and 3.6 mm-channels

The low range of pressure which is covered does not enable us to detect the variation of K with the pressure.

4.2 Change of the void fraction in subcooled boiling

4.2.1 Model

The empirical relationship defined in the preceding paragraph:

$$\theta = K.\varphi / \sqrt{V}$$

which links, at the time of appearance of vapor in the channel, the undersaturation θ, flux ϕ, and velocity V, can be considered as defining a coefficient of heat exchange between the vapor which is formed at the wall and the liquid core of the flow. When, because of the rise in temperature of the liquid or the pressure drop, the undersaturation becomes less than θ we will assume that there is a creation of a void α in the section which increases the velocity of the liquid and the surface of exchange between vapor and liquid so that locally the relationship

$$\theta = K\varphi / \sqrt{V}$$

This mechanism interprets the point of appearance of the vapor in subcooled boiling.

Let us specify the hypotheses.

Starting relationship: $\theta = K\,\varphi/\sqrt{V}$

$\theta = T_{sat} - T_L$

$$T_L \cong T - \frac{x\mathcal{L}}{C}$$

T = temperature of heat balance = $T_o + \int_o^z \frac{W_T(z)}{M.C}\,dz$

$\phi = W/B$

$W = W_T - W_V$

W_V = power absorbed by vaporization = $\mathcal{L}M\frac{dx}{dz}$

B = perimeter of exchange between water and vapor = $B_C\,(\delta + m\alpha)$

B_C = heated perimeter

$\delta = 1$ if $T_{colb} \geq T_{sat} + \Delta T_{FG}$

$\delta = 0$ if $T_{colb} < T_{sat} + \Delta T_{FG}$

α = void fraction in the section in consideration = $\dfrac{1}{1 + \dfrac{1-x}{x}\gamma}$

V = average velocity of the liquid = $\dfrac{M}{S.\rho_L}\;\dfrac{1-x}{1-\alpha}$

γ = slippage = $1 + n\alpha$

One then obtains the following differential relationship:

$$\frac{dx}{dz} = \frac{W_T}{M\mathcal{L}} - \frac{B_e(\delta + m\alpha)\,(T_{sat} - T_L)\sqrt{M\,(1-x)}}{K\sqrt{S\,\rho_L\,(1-\alpha)}\;M.\mathcal{L}}$$

4.2.2 Results

We calculated in a first step, longitudinal void profiles at constant pressure for reasons of simplicity of the calculations. Consequently, we will take into account the variations in momentum pressure, friction, and elevation. The comparison with the experimental results is therefore not strict because, in reality, no void profile is produced at constant pressure. This remark is also valid for the zone of condensation.

In Figure 10, we compared the measured void profiles with the calculated profiles for two cases at different pressures.

The agreement seems to be satisfactory between the model and the experiment, but it is necessary to note, nevertheless, that the start of the curve is more sudden for the calculated values than for the measured values and that it is the precision of the correlation which gives the point of departure which rules the precision of the calculations. Figure 11, which shows the variation of the void fraction in the course of recondensation, confirms the model since the calculated lengths of condensation are the same as the experimental lengths of condensation.

For these calculations, we have $B = B_C\ (1 + 2\alpha)$ and $\gamma = 1 + \alpha$ (see §4.2.1); this signifies that the surface of exchange increases proportionally with α and that the slippage is between 1 and 2 which corresponds to the currently accepted values in low pressure boiling.

4.2.3 Comparison with other models

Model of Lavigne [8]

The real titer x results from a local balance between: the vapor which is supplied + the vapor which enters - the condensed vapor = the vapor which leaves
the vapor supplied is

$$\left(1 - \frac{\Delta T}{\Delta T_S}\right) \frac{W_T}{\mathcal{L}} \quad dz$$

that is to say that the flux which vaporizes at the wall is zero at the beginning of subcooled boiling and W_T for $T = T_{sat}$.

The condensed vapor is: $\quad dm = K \frac{M}{V} \; x \; \Delta T \; dz$

The balance is then written:

$$\frac{dx}{dz} = \frac{W}{\mathcal{L} M} - \left(\frac{W}{\mathcal{L} \Delta T_S} + \frac{K x}{V}\right) \Delta T$$

It is suitable to use this model to determine the points of appearance of the subcooled boiling and the constant K.

In the model that we propose, it is the same value which gives the appearance and the change of the void.

Model of Bowring [6]

Bowring decomposes the local flux into three parts:

$$\phi = \phi_e + \phi_a + \phi_{SP}$$

ϕ_e = flux which vaporizes

ϕ_a = flux evacuated by agitation due to bubbles

ϕ_{SP} = flux evacuated by transfer in single phase

The author lets

$$\frac{\phi_a}{\phi_e}$$

and determines ε by experimentation.

In our case, ϕ_e results from the difference between the total flux supplied to the channel and the flux that the liquid evacuates.

Conclusion

From the tests performed, we obtained the following results:

- a correlation giving the conditions of appearance of vapor in subcooled boiling at low pressure with a negligible influence of the state of the surface of the channel, of the heated length, and of the dissolved gas content. The formula is $\theta = K\,\varphi/\sqrt{V}$

- a model of the void fraction in subcooled boiling tested in a first step by neglecting the variations of pressure but that we are going to perfect by taking into account the pressure drops by friction, elevation, and momentum and compare with other experimental results.

References

1. J. Costa, M. Courtaud, S. Elberg, J. Lafay, The redistribution of flow rate in the research reactors. Bulletin d'informations scientifiques et techniques du CEA 1967 (to appear).

[2] R. BORGAN - R.M. WHITTLE
Pressure drop characteritics for the flow of subcooled water at atmospheric pressure in narrow heated channels
Report A.E.R.E. M 1739 May 1966

[3] J.B. REYNOLDS
Local boiling pressure drop
Report A.N.L. 5178 March 1964

[4] W.L. OWENS - V.E. SCHROCK
Pressure gradients and heat transfer in forced convection boiling of subcooled water
Report T.I.D. 15078 June 1959

[5] G.B. ANDEEN and P. GRIFFITH
The momentum flux in two-phase flow
M.I.T. Report 3 496 - 1 (oct. 1965)

[6] R.W. BOWRING
Physical model, based on bubble detachment and calculation of steam voidage in the subcooled region of a heated channel
H.P.R 10 1962 88 pages

[7] N. ZUBER - F.W. STAUB and G. BIJWAARD
Vapor void fraction in subcooled boiling in an saturated boiling systems. U.S ASME n° 154
Third international heat transfer conference - August 7-12 1966 - Chicago, Illinois

8. P. Lavigne, Model of change of the titer and of the void fraction in subcooled boiling and zone of transition. C.E.A. Report No. 2365.

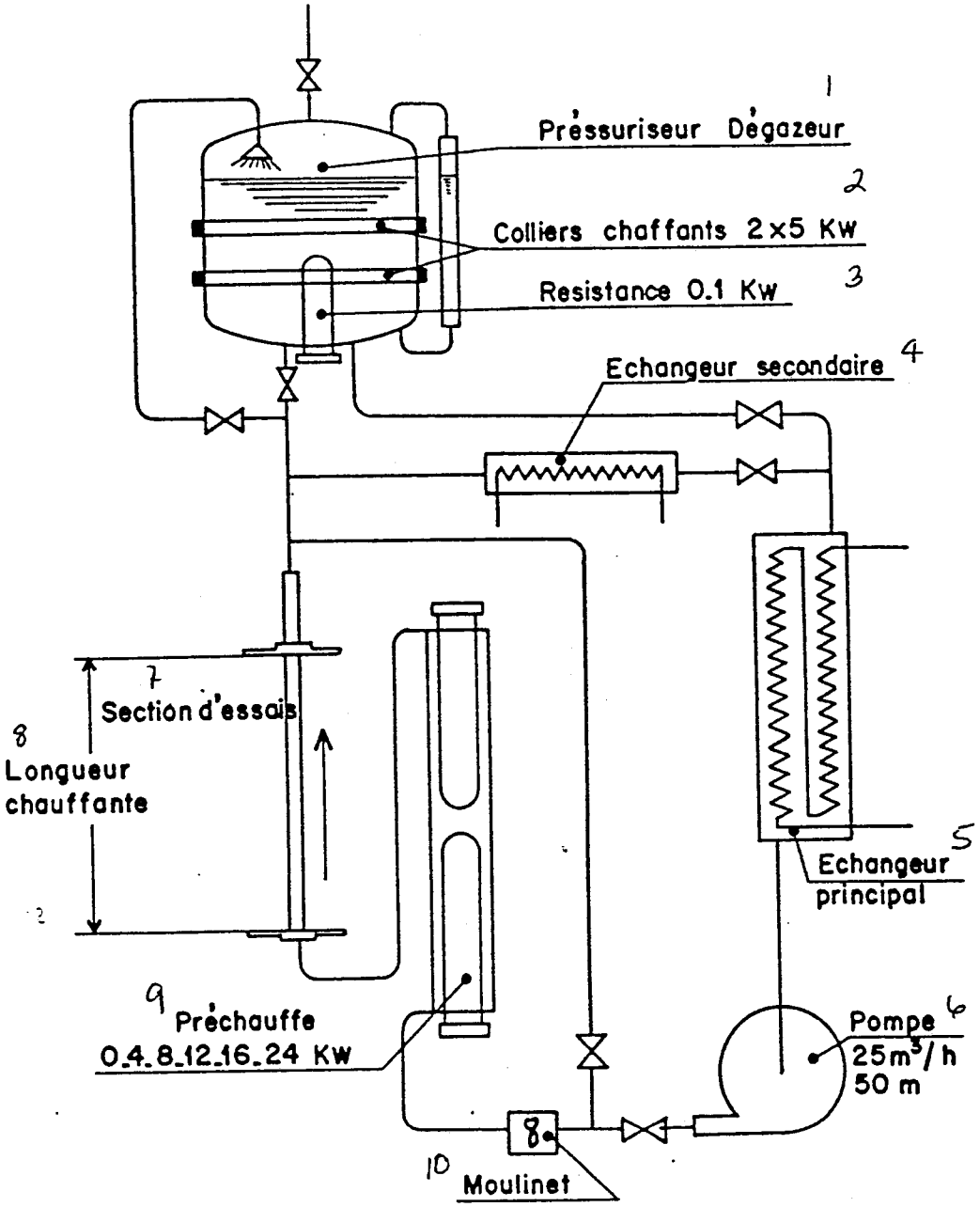

Figure 1. Diagram of the loop

Key to Figure 1:

1 - Degasser pressurizer
2 - Heating bands 2 x 5 kW
3 - Resistance 0.1 kW
4 - Secondary exchanger
5 - Principal exchanger
6 - Pump
7 - Test section
8 - Heated length
9 - Preheating
10 - Turnstile winch

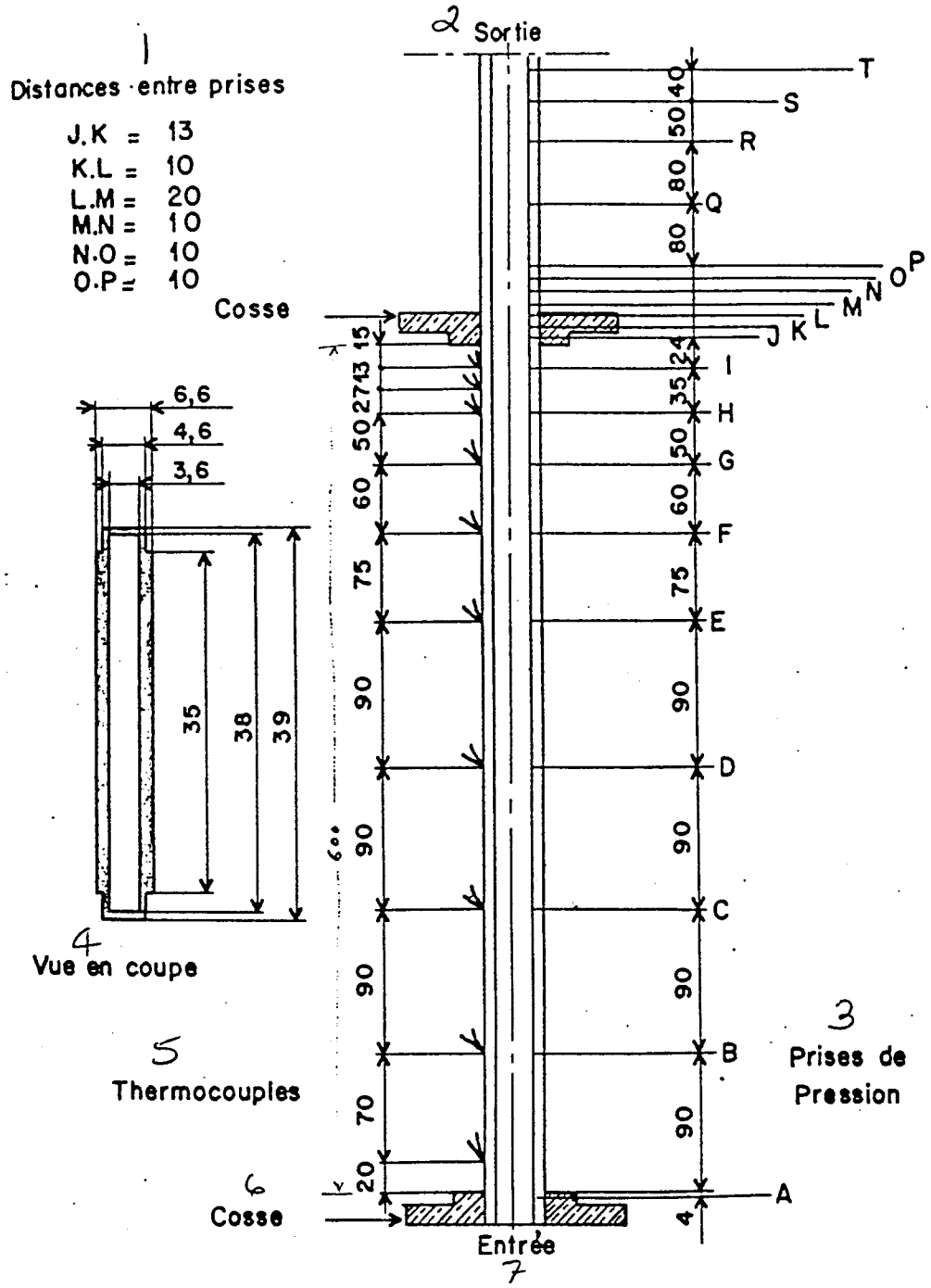

Figure 2. Diagram of the test section.

Key to Figure 2:

1 - Distances between outlets
2 - Output
3 - Pressure outlets
4 - Cross section
5 - Thermocouples
6 - Terminal
7 - Entrance

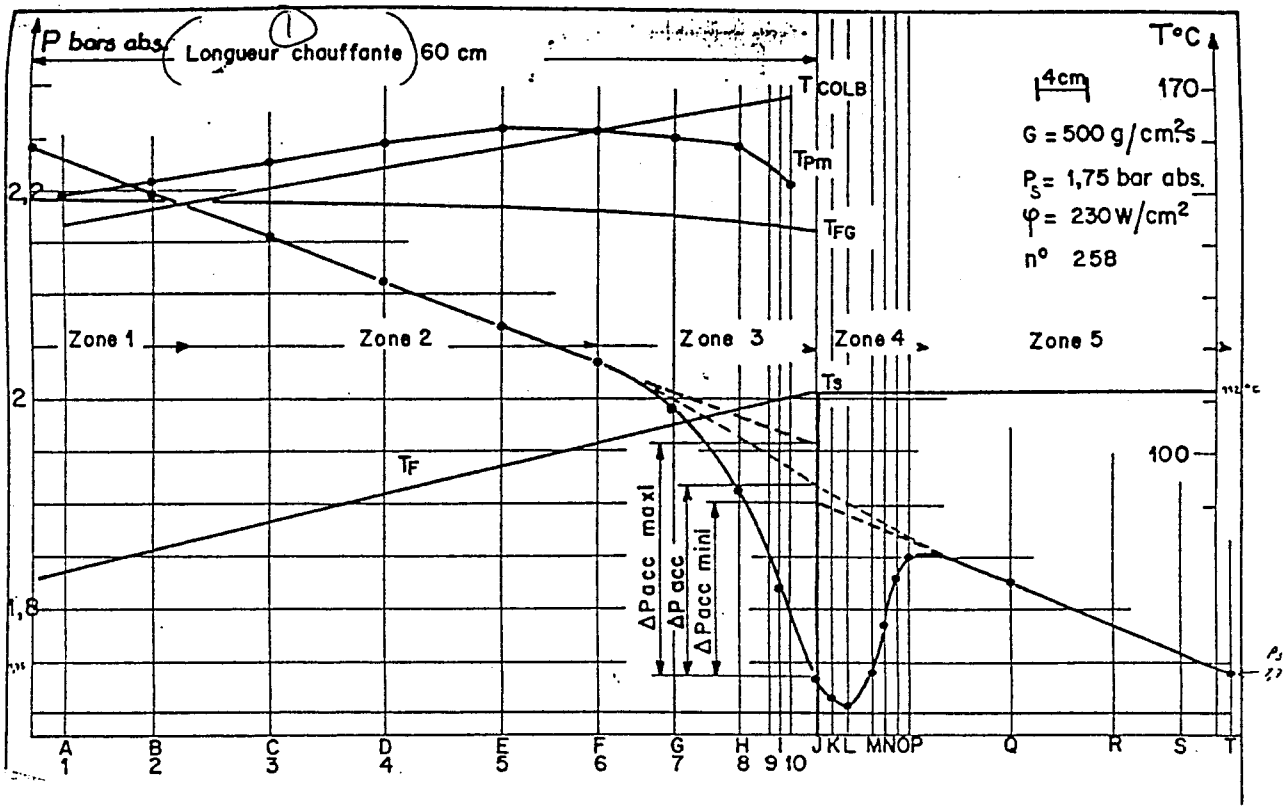

Figure 3. Piezometric line in subcooled boiling.
Channel ▭ 3.6 mm x 38 mm

Key:
1 - Heated length

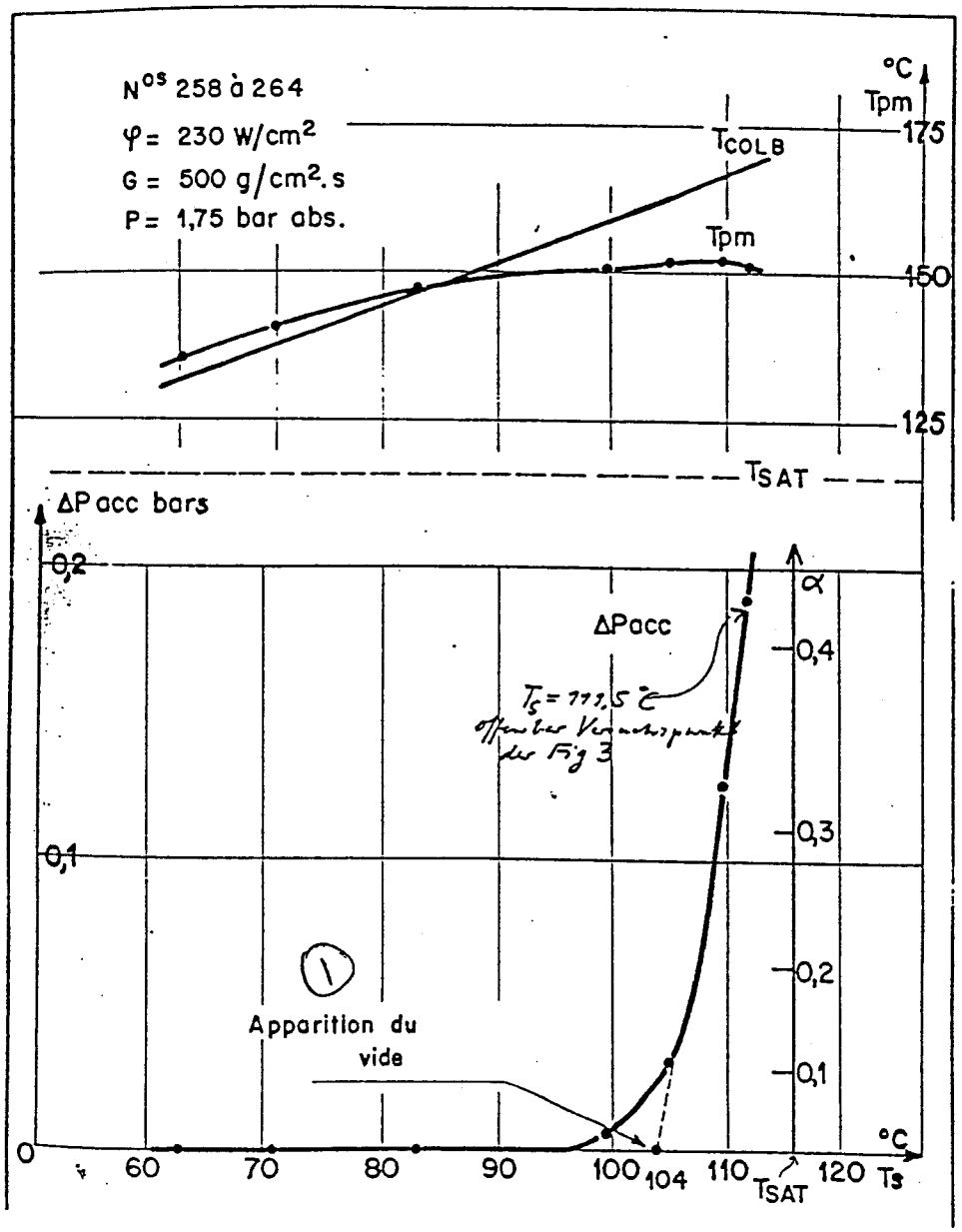

Figure 4. Appearance of the momentum pressure drop in subcooled boiling. Rectangular channel 3.6 mm.

Key:
1 - Appearance of the void

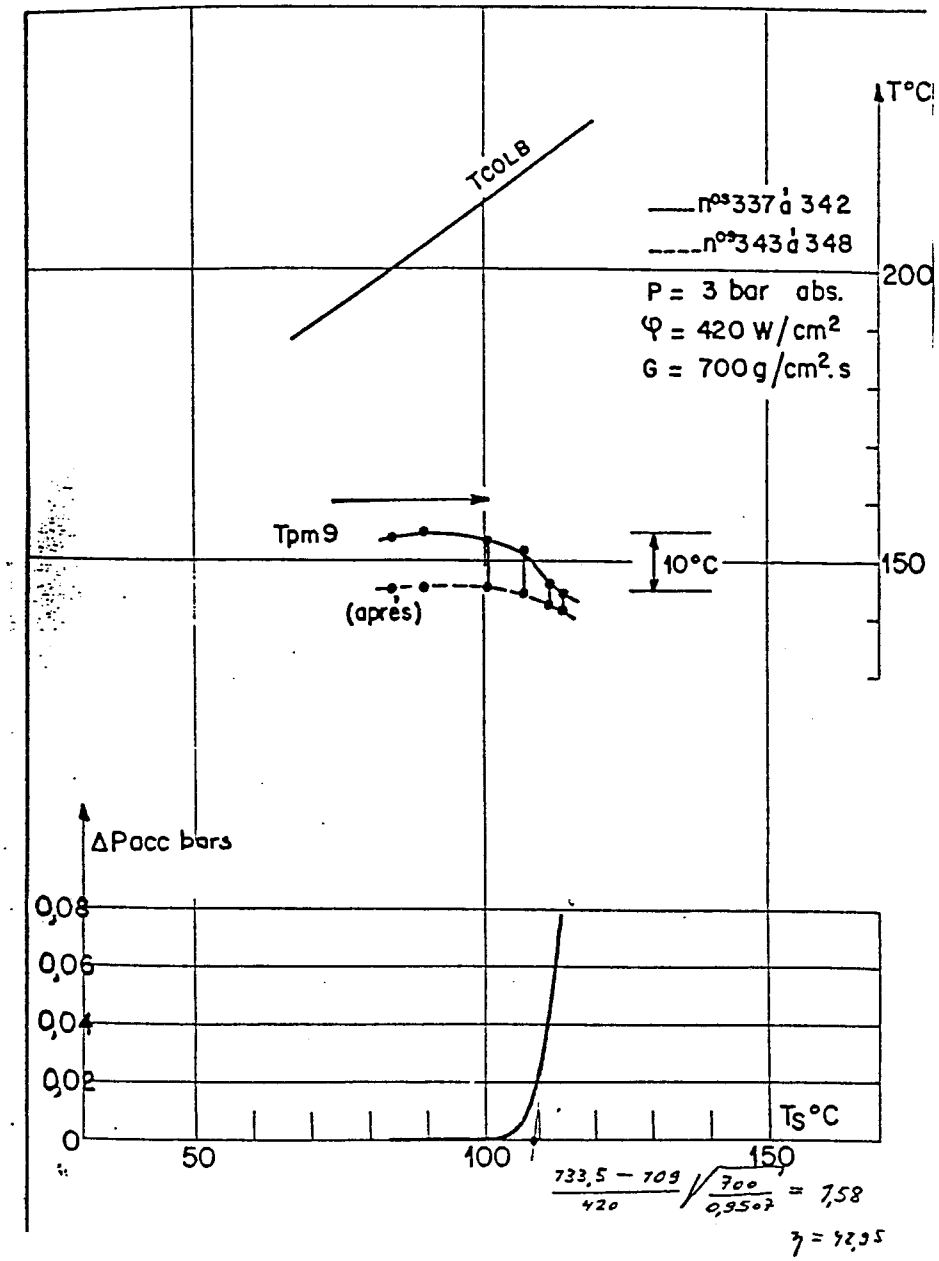

Figure 5. Influence of the state of the surface of the channel 6 mm ϕ.

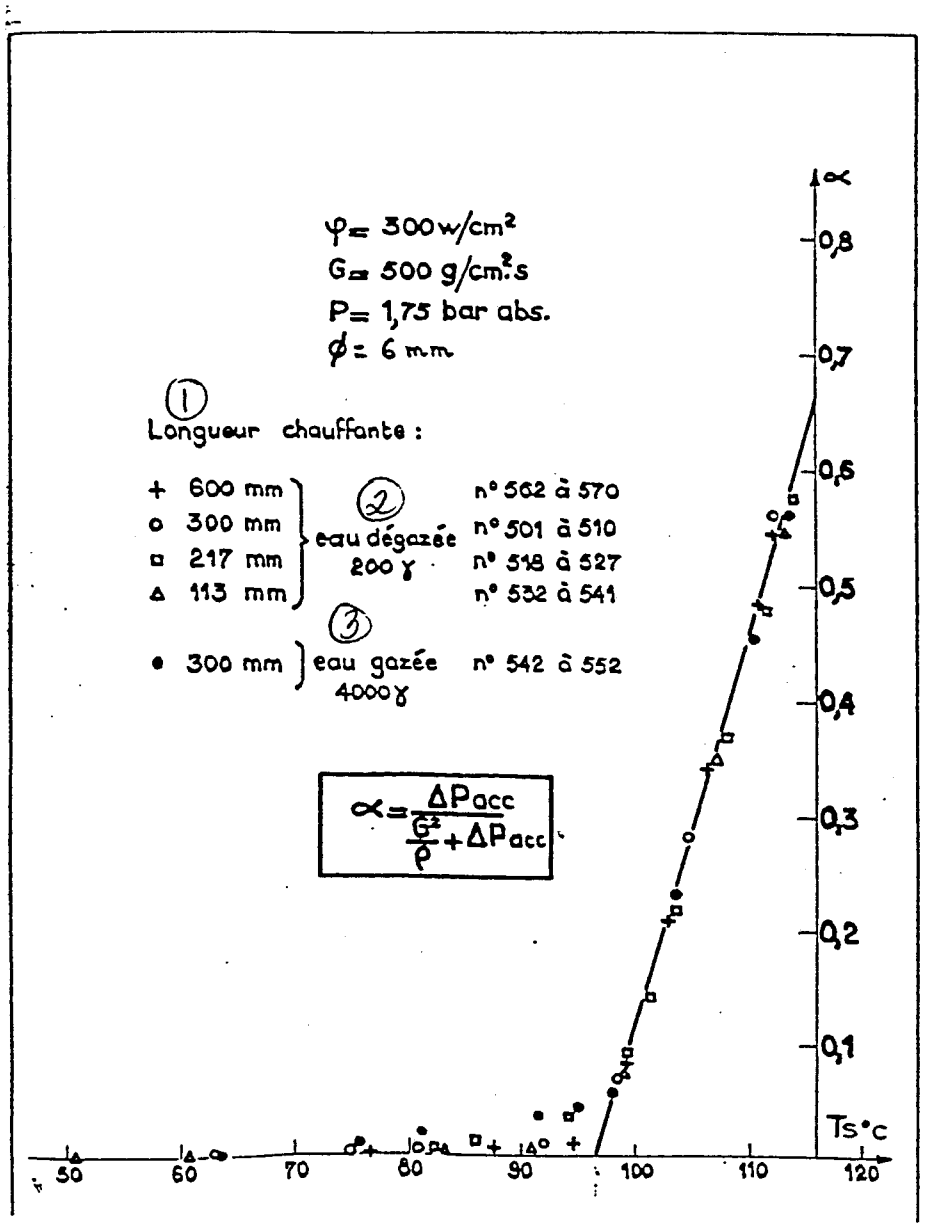

Figure 6. Influence of the heated length and of the gas content.

Key:
1 - Heated length
2 - Degassed water
3 - Gassed water

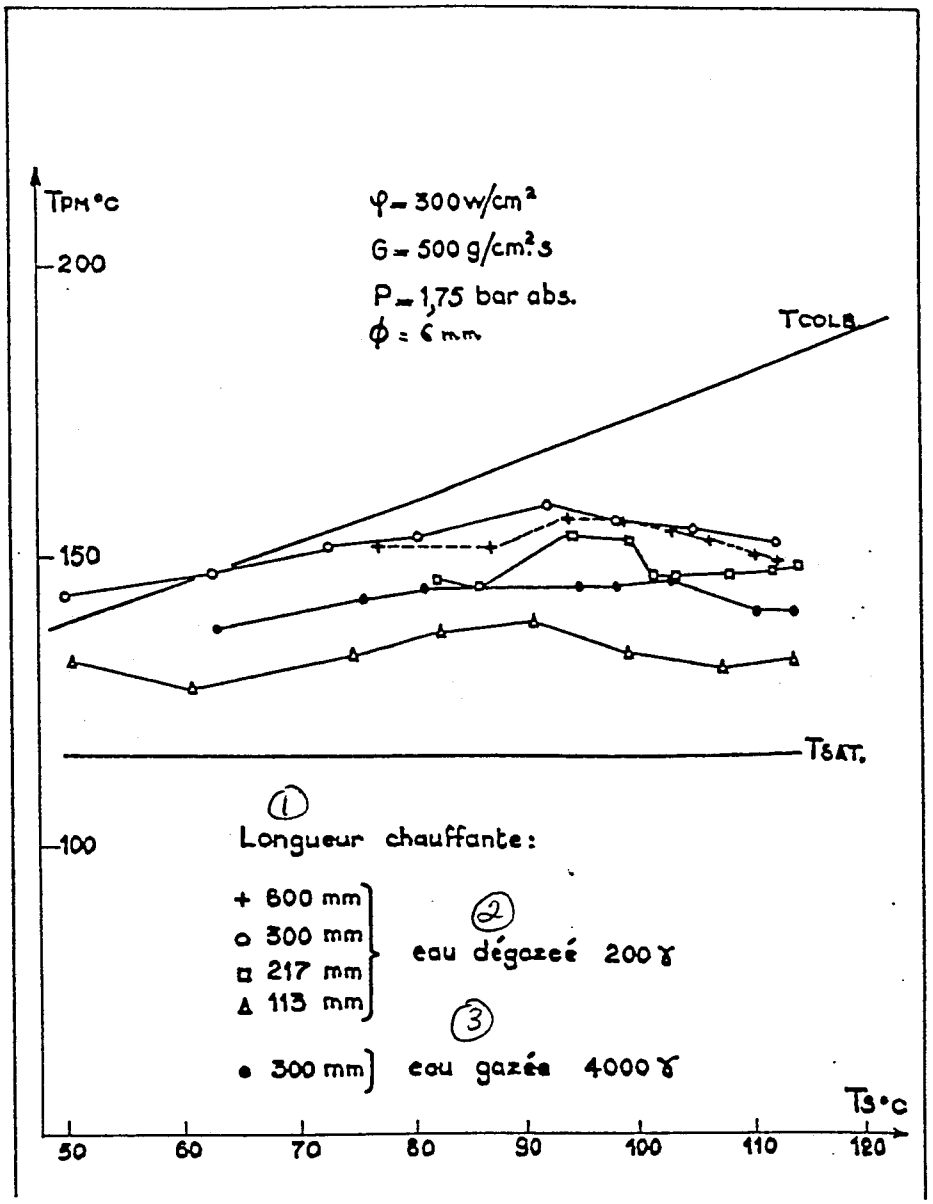

Figure 7. Influence of the heated length and of the gas content.

Key:
1 - Heated length
2 - Degassed water
3 - Gassed water

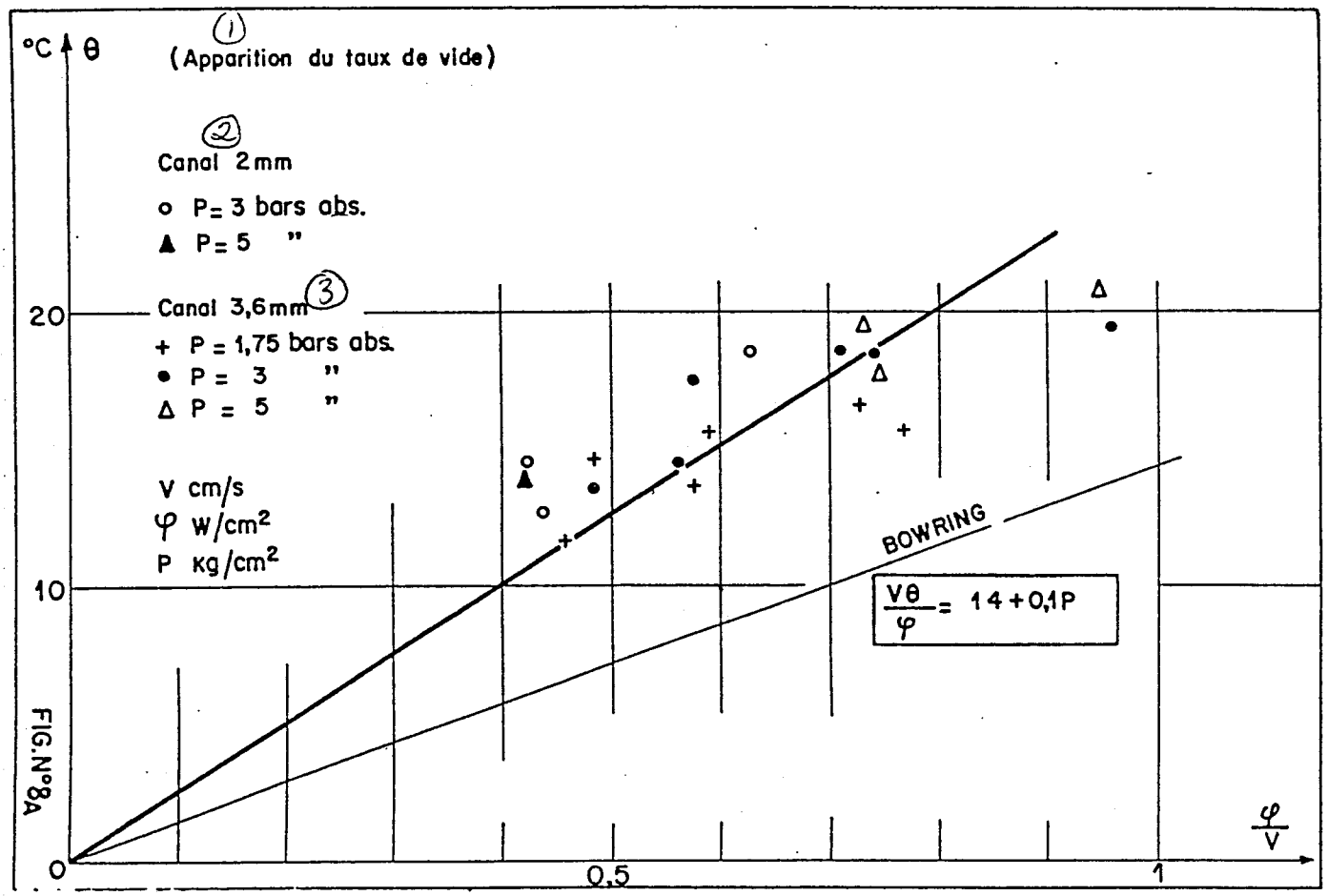

Figure 8A. Comparison of the results with the Bowring formula.

Key:
1 - (Appearance of the void fraction)
2 - 2-mm channel
3 - 3.6-mm channel

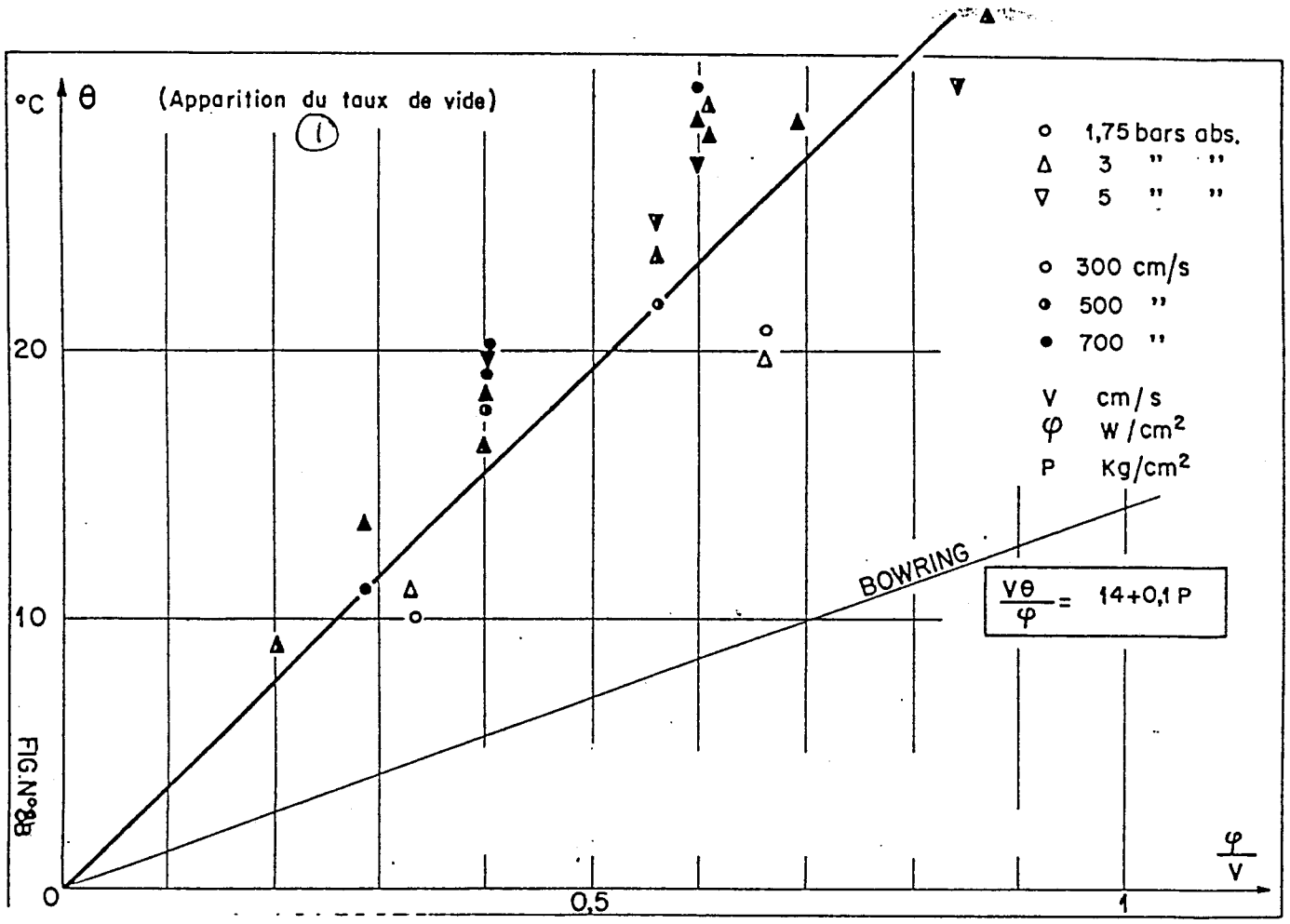

Figure 8B. Comparison of the results with the Bowring formula.

Key:
1 - (Appearance of the void fraction)

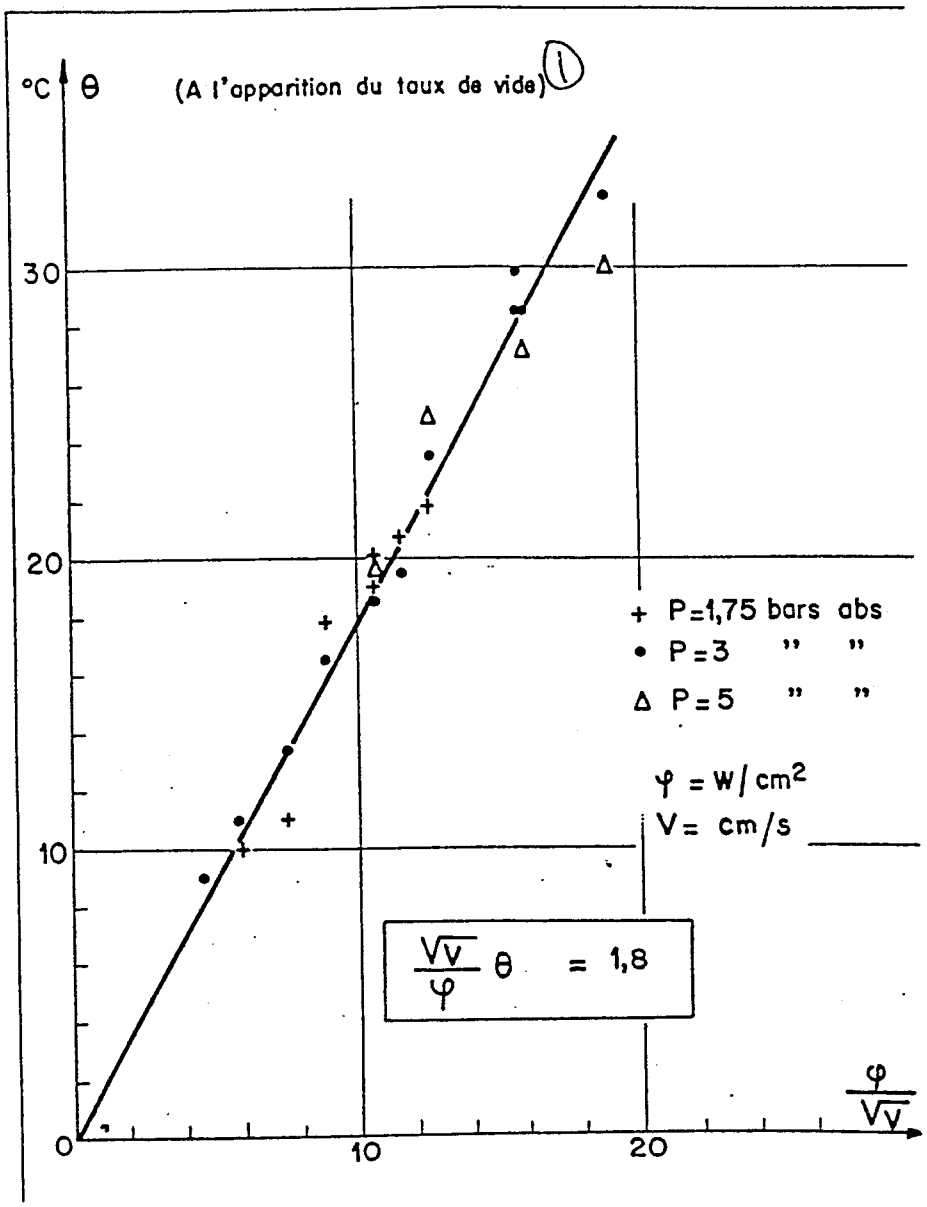

Figure 9A. Experimental results. Circular channel 6 mm ϕ.

Key:
1 - (At the appearance of the void fraction)

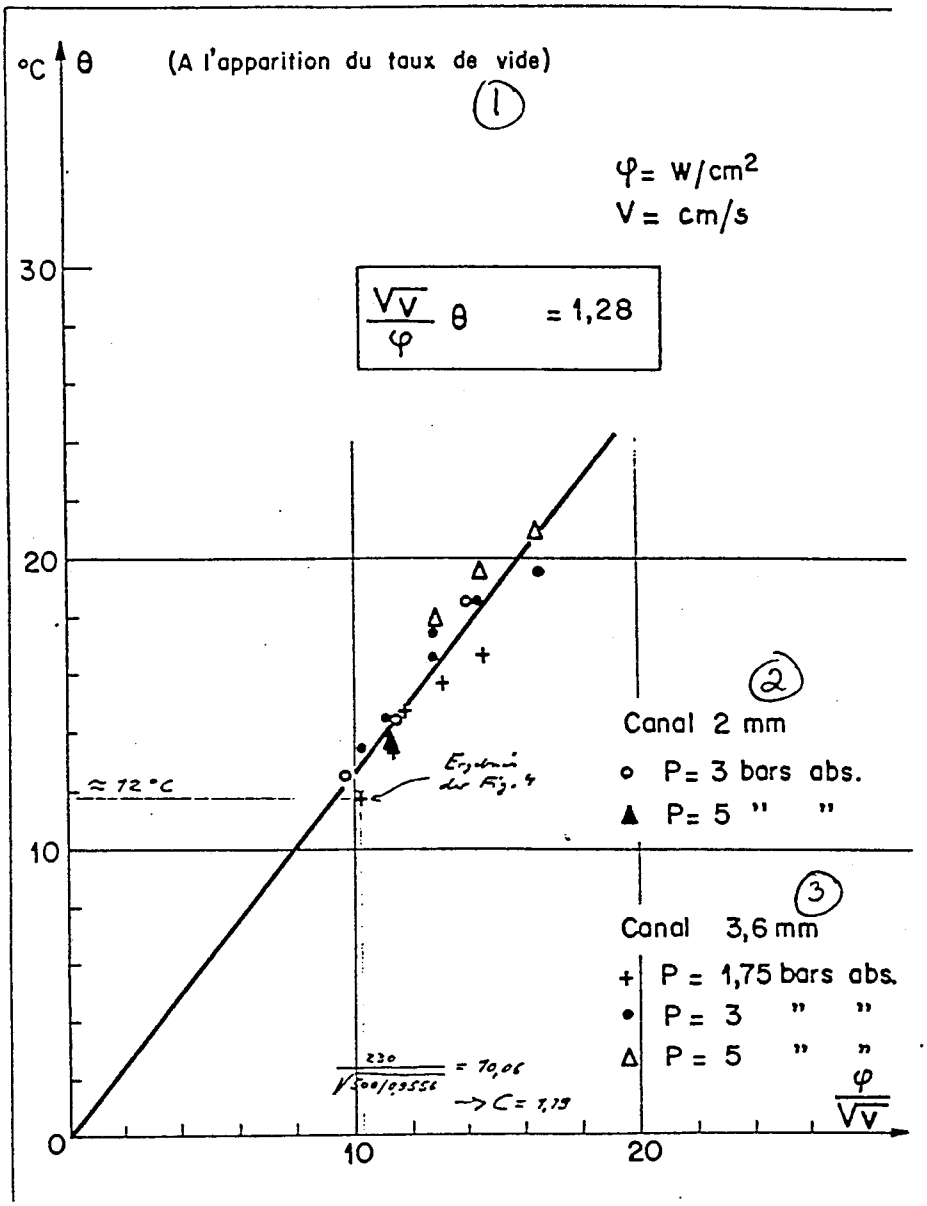

Figure 9B. Experimental results.
Rectangular channels 2 and 3.6 mm.

Key:
1 - (At the appearance of the void fraction)
2 - 2-mm channel
3 - 3.6-mm channel

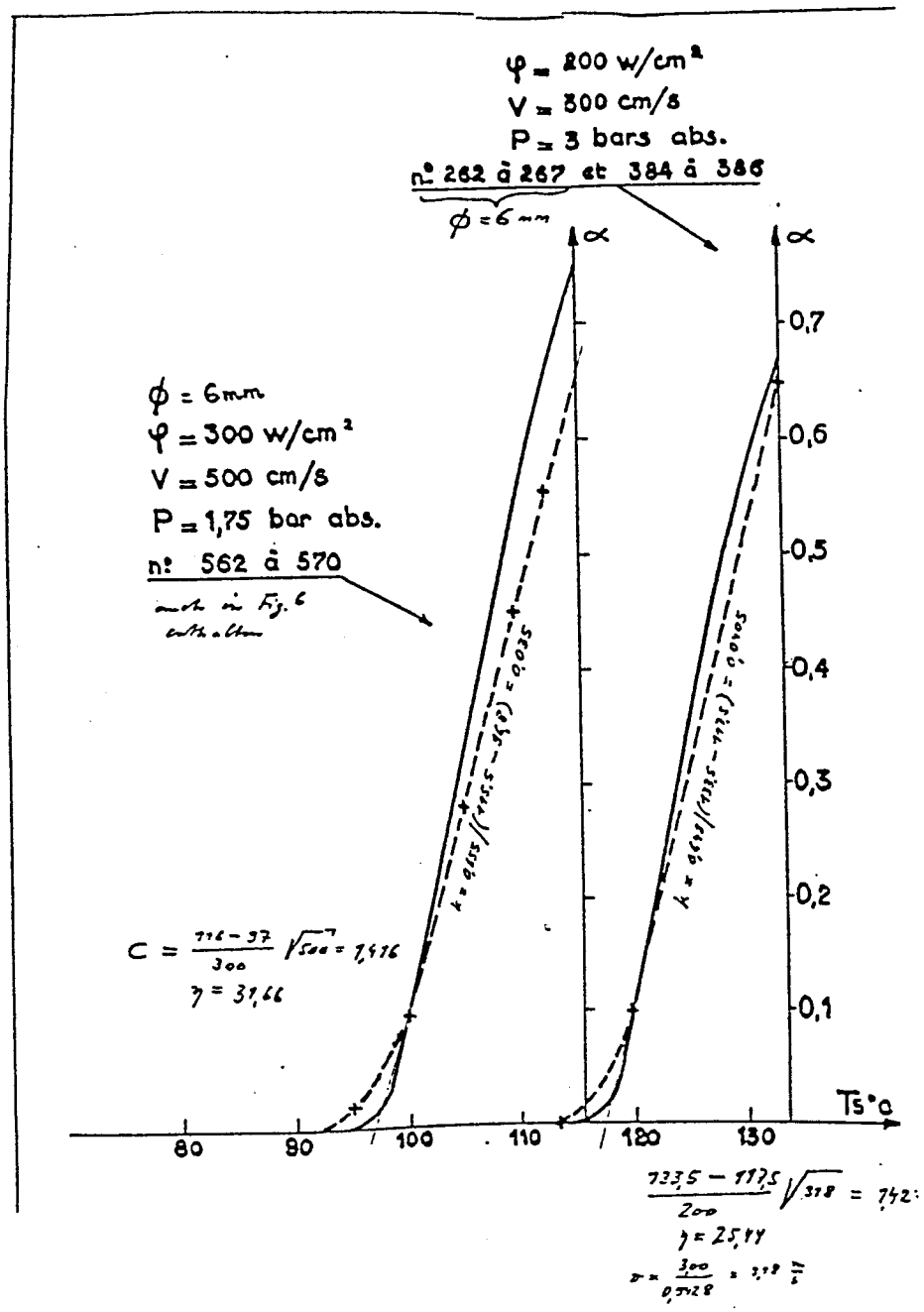

Figure 10. Void profile
Measured ------
Calculated _____

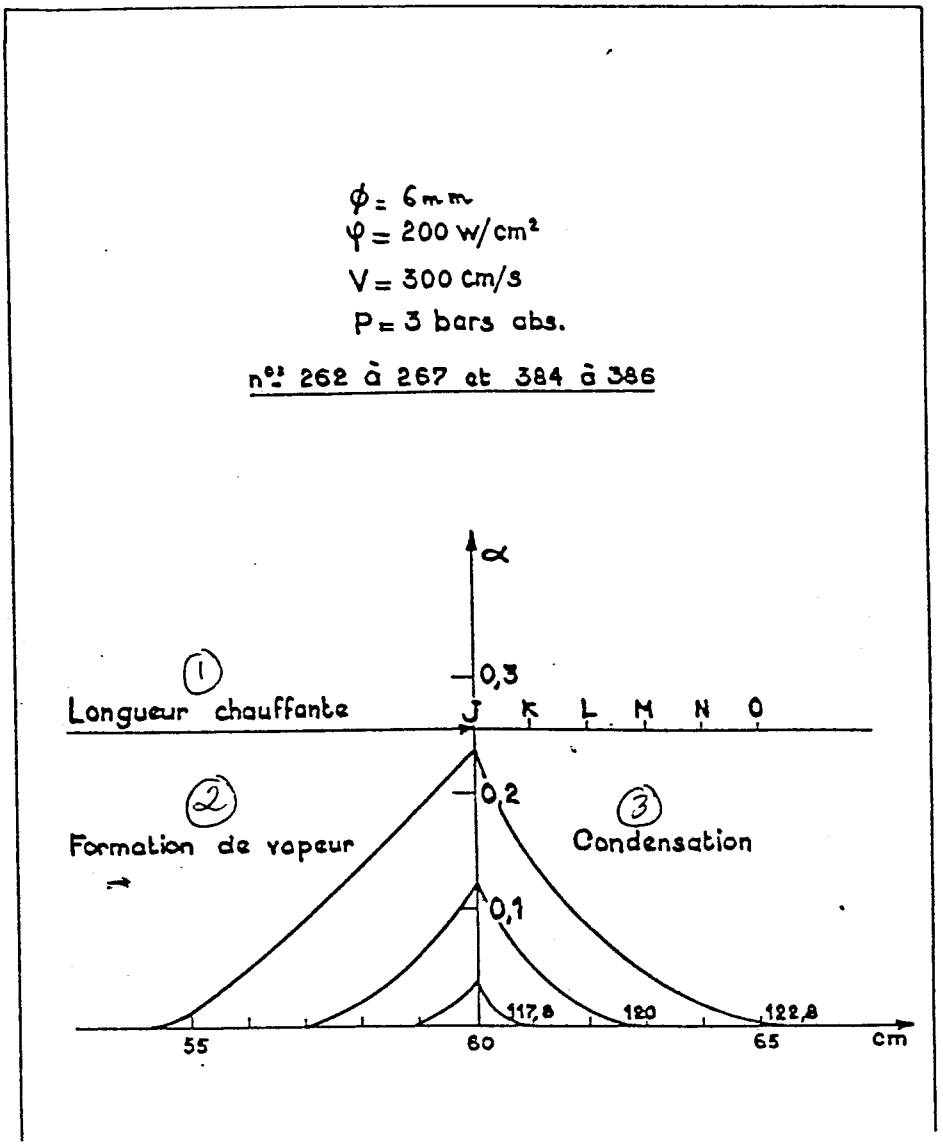

Figure 11. Condensation at the end of the heated length.

Key:
1 - Heated length
2 - Formation of vapor
3 - Condensation

Table I. Results concerning the point of appearance of the void fraction in subcooled boiling.

T_F = Fluid-Temperature bei Entstehung der Dampfblasen ?

(1) Canal rectangulaire de 38 x 2 mm

N° (2) essais	P (bars abs)	φ (W/cm²)	G g/cm².s	T_F °C
374 à 379	2,985	314	745	119
380 à 385	2,985	314	500	115
386 à 391	2,985	218	500	121
392 à 397	4,985	310	750	138

(3) Canal rectangulaire de 38 x 3,6 mm

N° (2) essais	P (bars abs)	φ (W/cm²)	G g/cm².s	T_F °C
217 à 221	2,985	220	455	120
222 à 226	2,985	222	300	117
228 à 232	2,985	287	500	116
233 à 238	2,985	287	405	115
240 à 244	4,985	284	590	132,3
245 à 250	4,985	284	300	131
252 à 257	1,735	293	497	100 *
258* à 264	1,735	229	502	104
266 à 271	1,735	228	397	102
272 à 276	1,735	229	300	100
278 à 282	1,735	290	398	99
283 à 288	4,985	225	300	134
289 à 294	2,985	225	400	119
296 à 301	1,735	290	600	101
302 à 305	2,985	287	300	114

* zeigt, daß T_F die Temper. bei Entstehen Blasen ist.

Key:
1 - Rectangular 38 x 2 mm channel
2 - Test No.
3 - Rectangular 38 x 3.6 mm channel

Table I (continued)

Canal circulaire ∅ 6 mm (1)

N° essais (2)	P (bars abs)	φ (W/cm²)	G (g/cm².s)	T_F °C
208 à 222	2,985	360	520	105
230 à 235	2,985	420	690	105,5
236 à 239	2,985	420	490	101
240 à 245	2,985	280	500	110
246 à 251	2,985	280	700	115
252 à 256	2,985	200	700	120
257 à 261	2,985	200	500	117
262 à 267	2,985	200	300	114? mes Fig. 7b
268 à 274	2,985	100	495	124,5
281 à 285	1,740	416	695	86
286 à 291	1,740	280	695	96,8
292 à 298	1,740	280	695	95,8
297 à 304	4,985	280	695	132
305 à 310	4,985	280	498	127
311 à 315	1,740	280	498	96
316 à 321	1,740	200	700	105
322 à 327	1,740	200	500	98
328 à 330	1,740	200	300	95
331 à 335	1,740	100	300	106
337 à 342	2,985	420	700	105? 103
343 à 348	2,985	420	700	105? 103
349 à 354	2,985	100	300	122,5
355 à 360	4,985	420	700	125
361 à 364	4,985	420	500	122

Key:
1 - Circular channel 6 mm ϕ
2 - Test No.